

# MODELLING OF SILICA BREAKTHROUGH IN WELL PN-26 PALINPINON, PHILIPPINES

R.C.M. Malate M.J. O'Sullivan

Engineering Science Department, University of Auckland

## Abstract

Production silica changes observed in well PN-26 are modelled by coupling the silica mass balance model for the production area to a transport and deposition model for the fractured zone which connects the reinjection and production sectors. The results of the model further validate the results obtained from the chloride and temperature models developed earlier by the authors. That is, a large fraction of the reinjected fluid returns to the production sector.

## Introduction

Chloride and temperature changes for well PN-26 have been modelled previously by Malate and O'Sullivan (1990) using a simple production-reinjection lumped parameter model. In this paper, the model is extended to simulate the observed changes in production silica for the well.

Despite the large increase in production chloride concentration, in response to the rapid return of reinjection (RI) fluid, silica concentration for well PN-26 remained constant for the first two years of continuous exploitation (Figure 1). This means that the RI fluid, supersaturated with silica (quartz) must have deposited it in the reservoir and then rapidly equilibrated with respect to quartz at the production temperature. Increased levels of silica (silica breakthrough) in the PN-26 produced fluid were only observed in the succeeding years. The term "silica breakthrough" is used to describe the situation when the silica concentrations in the produced fluid are no longer governed by quartz solubility (Harper, 1986). In other words, the reservoir silica concentration is found to be higher than the corresponding quartz saturation at the measured temperature and pH.

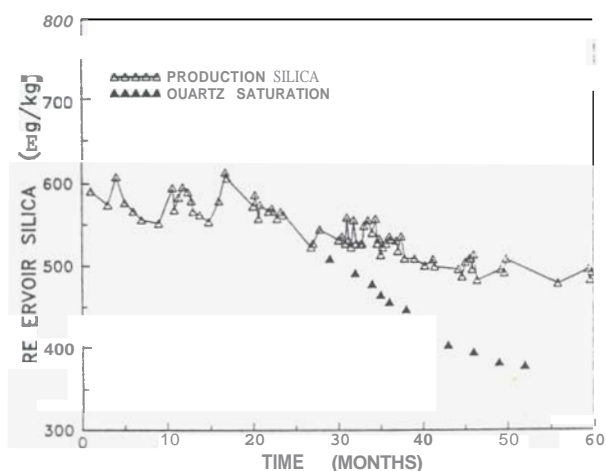


Fig.1 Well PN-26 Reservoir Silica vs Time

During the same interval, well PN-26 also showed a temperature decrease of approximately 38°C, from its baseline temperature of 280°C down to 242°C, measured at the main production zone, 1600m CHF (see Figure 2). The calculated silica temperature (TSiO<sub>2</sub>) based on quartz geothermometry is also presented in Figure 2. The silica temperature was in close agreement with the measured temperature for the first two years but was higher than the measured temperature after silica breakthrough.

Amistoso and Torrejos (1986) reported that the thermal decline in PN-26 was accompanied by a mass flow decline. This was interpreted to have resulted mainly from the cooling effect of RI fluid.

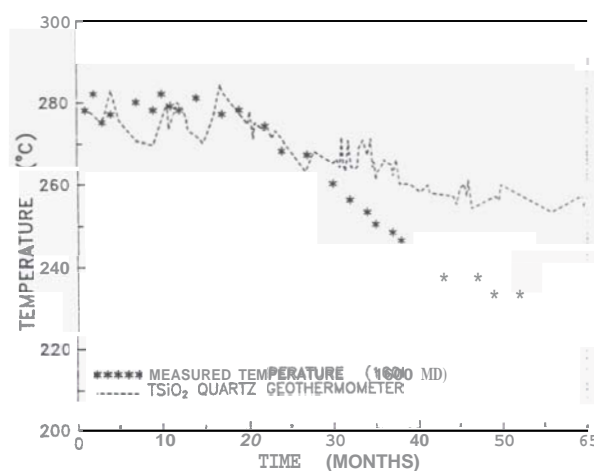


Fig. 2 Well PN-26 Measured Temperature vs Time

A plot of reservoir silica concentration against the measured temperature at the major production zone is shown in Figure 3. It can be seen that silica breakthrough has continued as the measured temperature has declined, the difference between the two becoming more pronounced.

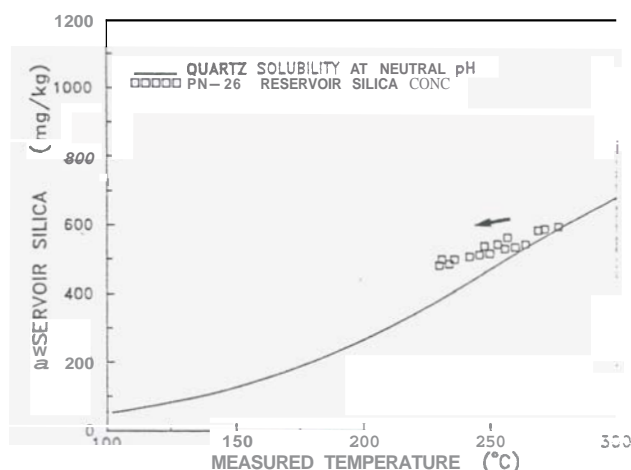


Fig.3 Reservoir Silica vs Measured Temperature

If it is assumed that the silica content is controlled by quartz solubility, it is evident that the silica being returned by the reinjection fluid has not fully re-equilibrated with quartz. In such a re-equilibration, the kinetics of silica is important. A significant shift in reservoir pH due to exploitation could also account for the deviation of reservoir silica concentration. However, the rocks, especially feldspar, would buffer a shift in fluid pH. Therefore for the purposes of this discussion, the effect of reservoir pH is considered to be negligible.

### Lumped Parameter Model

The lumped parameter model used here consists of a production sector and a reinjection sector connected by a high permeability fractured zone. The same model was used previously by Malate and O'Sullivan (1990) to model changes in the production chloride content and temperature for PN-26. This was achieved by setting up chloride balance and energy balance equations for the production sector and coupling them to a simple chemical and heat transport model for the fractured zone. In the present work the changes in production silica concentration are also modelled by coupling a silica mass balance model for the production sector to a transport and deposition model for the fractured zone (see Figure 4). The first order kinetic equation for silica (quartz) deposition suggested by Rimstidt and Barnes, 1980, is used in both the production sector and the fractured zone.

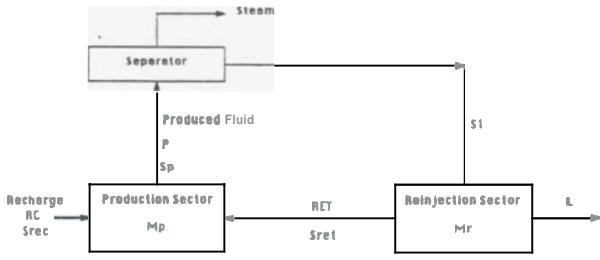


Fig. 4 Production-Reinjection Lumped Parameter Model

A silica mass balance for the production sector gives

$$\frac{d}{dt} M_p S_p = RC S_{rec} + RET S_{ret}(t) - P S_p - k M_p (S_p - S_s) \quad (1)$$

where  $M_p$  is the mass of fluid in the production area,  $RC$  is the recharge flow to the production zone,  $RET$  is the flow of RI fluid back to production zone and  $P$  is the production rate. The symbols  $S_p$ ,  $S_{rec}$  and  $S_{ret}$  refer to the silica mass fraction of the production, recharge and returning fluid respectively. The kinetic effect is represented by the last term in equation (1) where  $S_s$  is the silica (quartz) saturation and  $k$  is the precipitation constant.

Here,  $k = k^- \left( \frac{A}{M} \right)_p$  where  $k^-$  is the apparent precipitation rate constant and  $\left( \frac{A}{M} \right)_p$  is the ratio of the surface area to the mass of the fluid available in the production area.

The initial conditions used are  $S_p(0) = S_{p0}$  and  $S_{rec}(0) = S_{p0}$  where  $S_{p0}$  is the initial reservoir silica concentration. To simplify the equations, the change in silica concentration is used in the form:

$$\Phi_p = S_p - S_{p0} \text{ and } \Phi_{ret} = S_{ret} - S_{p0}.$$

Then (1) becomes

$$M_p \frac{d\Phi_p}{dt} = -(P + k M_p) \Phi_p + RET \Phi_{ret}(t) - k M_p (S_{p0} - S_s) \quad (2)$$

and the transformed initial condition is  $\Phi_p(0) = 0$ . Rearranging and simplifying equation (2) gives

$$\frac{d}{dt} \Phi_p + \lambda \Phi_p = \gamma \Phi_{ret}(t) - F(t) \quad (3)$$

$$\text{where } \lambda = \left( \frac{P}{M_p} + k \right), \quad \gamma = \frac{RET}{M_p} \text{ and } F(t) = k(S_{p0} - S_s).$$

Before (3) can be solved the functions  $F(t)$  and  $\Phi_{ret}(t)$  must be evaluated. The function  $F$  varies with temperature because the quartz silica saturation  $S_s$  changes with production sector temperature. By making some approximations,  $F$  can be evaluated in a simple form thus enabling (3) to be solved analytically. In particular, the rate constant  $k$  is assumed not to vary appreciably for the range of temperatures considered and the silica saturation concentration is approximated by a quadratic function. Then the silica saturation concentration is given by:

$$S_s = S_{p0} \quad \text{for } t < t_T \quad (4)$$

and

$$S_s = S_{p0} - d_1 (T_0 - T_p) - d_2 (T_0 - T_p)^2 \quad \text{for } t > t_T \quad (5)$$

where  $T_0$  is the initial reservoir temperature and  $U$  is the velocity of the thermal front. The thermal front is the transition zone where the temperature changes from the initial reservoir temperature  $T_0$  to the injection temperature  $T_1$ . The velocity  $U$  is defined by

$$U = \frac{V \phi \rho_r c_r}{[(1 - \phi) \rho_r c_r + \phi \rho_f c_f]}$$

and  $t_T$ , the time taken for the thermal front to travel the distance  $L$ , is defined by

$$t_T = \frac{L}{U}.$$

Here  $V$  is the fluid particle velocity,  $\phi$  is porosity,  $\rho_r$  and  $c_r$  are the density and specific heat of the rock and  $\rho_f$  and  $c_f$  are the density and specific heat of the fluid. Note that  $V$  is also the "silica front" velocity as the silica moves with the water. The temperature in the production sector is given by (Malate and O'Sullivan, 1990):

$$T_p = T_0 \quad \text{for } t < t_T \quad (6)$$

and

$$T_p = T_0 + W \{1 - \exp[-a(t - t_T)]\} \quad \text{for } t > t_T \quad (7)$$

$$\text{where } W = \frac{c}{a} (T_1 - T_0).$$

The parameters  $a$  and  $c$  are evaluated from  $a = \frac{P}{[M_p(1 + \beta)]}$  and

$$c = \frac{RET}{[M_p(1 + \beta)]}, \quad \text{where } \beta = \frac{(1 - \phi) \rho_r c_r}{\phi \rho_p c_p}$$

Here  $\rho_p$  and  $c_p$  are the density and specific heat of the fluid in the production sector. Then (5) can be simplified using the temperature from (7):

$$S_{p0} - S_s = m_0 + m_1 \exp(-at) + m_2 \exp(-2at) \quad (8)$$

$$\text{where } m_0 = (-d_1 + d_2 W) W, \quad m_1 = (d_1 - 2d_2 W) W \exp(at_T) \text{ and } m_2 = d_2 W^2 \exp(2at_T).$$

### Fracture Model

In this section the fractured zone is investigated and a solution for  $\Phi_{ret}(t)$  is obtained. For the present problem of non-isothermal flow through the fractured zone, the solution for silica concentration derived by Malate and O'Sullivan (1988) for the isothermal case is coupled with the temperature solution for the returning fluid. The solution for  $T_p$  given in (6) and (7) is based on a uniform porous medium model for the fractured zone with the temperature of the RI fluid given by:

$$T_f = T_1 \quad \text{for } x < Ut \quad (9)$$

and

$$T_f = T_0 \quad \text{for } x > Ut \quad (10)$$

The silica concentration in the fractured zone is governed by the transport equation

$$\frac{\partial S}{\partial t} + V \frac{\partial S}{\partial x} = -Re. \quad (11)$$

Assuming first order kinetics, the deposition rate  $Re = k(S - S_s)$ . Then the silica concentration solution for the isothermal case is

$$S = S_s + (S_1 - S_s) \exp \left( -\frac{kx}{V} \right) \quad \text{for } x < Vt \quad (12)$$

$$S = S_s \quad \text{for } x > Vt \quad (13)$$

where  $S_1$  is the concentration of silica in the injected water.

The procedure for solving (11) for the coupled problem using the method of characteristics, is presented diagrammatically in Figure 5. The silica front moves faster than the thermal front, therefore  $V > U$ . Since the temperature influences the thermodynamic and kinetic properties of the fluid, the characteristic curves required for solving the silica transport equation also depend on temperature. The figure shows three distinct solution regions:

- (i) A region at the injected fluid conditions (Region I,  $x < Ut$ )
- (ii) A region at the injected fluid silica concentration but still at the initial temperature (Region II,  $Ut < x < V_0 t$ ).
- (iii) A region still at the initial state (Region III,  $x > V_0 t$ ).

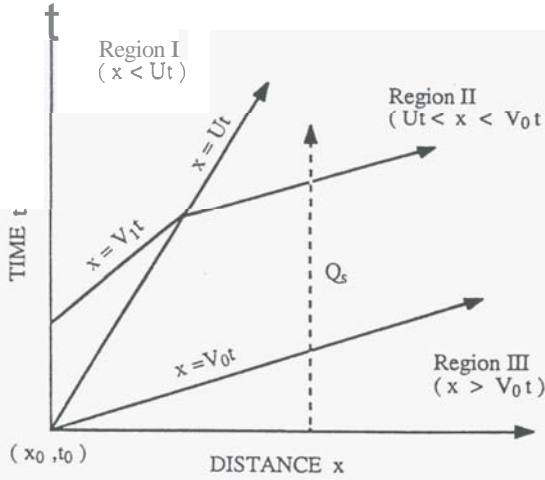


Fig. 5 Time-Distance diagram for the Silica Concentration.

The solution for the silica concentration in the fractured zone then can be expressed as follows:

**Region I** ( $x < Ut$ )

$$S_f = S_{s1} + (S_1 - S_{s1}) \exp\left(\frac{-k_1 x}{V_1}\right) \quad (14)$$

**Region II** ( $Ut < x < V_0 t$ )

$$S_f = S_{s0} + (S_{s1} - S_{s0}) \exp[\tau(x - Ut)] + (S_1 - S_{s1}) \exp\left[\frac{\sigma x + \omega t}{\delta}\right] \quad (15)$$

**Region III** ( $x > V_0 t$ )

$$S_f = S_{s0} \quad (16)$$

$$\text{Here } \tau = \frac{k_0}{(U - V_0)}, \quad \sigma = [k_0 V_1 - k_1 U],$$

$$\omega = U[k_1 V_0 - k_0 V_1] \quad \text{and} \quad \delta = V_1 (U - V_0).$$

The subscripts (1) and (0) refer to the conditions at temperatures  $T_1$  and  $T_0$  respectively. Here  $k_1 = k_1^- \left(\frac{A}{M}\right)_f$  and  $k_0 = k_0^- \left(\frac{A}{M}\right)_f$

where  $\left(\frac{A}{M}\right)_f$  is the ratio of surface area to the mass of fluid in the fractured zone. The amount of silica deposited in the fractured zone can be evaluated from the deposition equation

$$\frac{\partial Q_s}{\partial t} = \frac{\phi \rho_s}{(1 - \phi_0) \rho_s} k(S - S_s). \quad (17)$$

Here  $\phi_0$  is the initial porosity and  $\rho_s$  is the density of deposited silica. Malate and OSullivan (1988) have shown how to solve (17) for the isothermal case. Following a similar procedure for the present non-isothermal case (see Fig. 5) the solution for silica deposition  $Q_s$  is obtained as follows:

**Region III** ( $x > V_0 t$ )

$$Q_s = Q_{s0} \quad (18)$$

**Region II** ( $Ut < x < V_0 t$ )

$$Q_s = Q_{s0} + \frac{\phi_0}{\alpha} [1 - \exp(f(x, t))] \quad (19)$$

where

$$f(x, t) = \xi_0 \alpha \left\{ M_3 - M_1 \exp\left[\frac{\sigma x + \omega t}{\delta}\right] + M_2 \exp[\tau(x - Ut)] \right\}.$$

Here  $Q_{s0}$  is the initial mass fraction of deposited silica in the fractured zone. Also

$$\alpha = \frac{(1 - \phi_0) \rho_r}{(1 - \phi_s) \rho_s} \quad \text{and} \quad \xi_0 = \frac{\rho_{s0} k_0}{(1 - \phi_0) \rho_r}$$

where  $\phi_s$  is the density of deposited silica.

The constant  $M_3$  is evaluated from  $M_3 = (M_1 - M_2) \exp\left(\frac{-k_0 x}{V_0}\right)$ ,

where  $M_1 = \frac{6}{\omega} (S_1 - S_{s0})$  and  $M_2 = \frac{1}{TU} (S_{s1} - S_{s0})$ .

**Region I** ( $x < Ut$ )

$$Q_s = Q_{s0} + \frac{\phi_0}{\alpha} [1 - \exp(g(x, t))] \quad (20)$$

where

$$g(x, t) = \xi_0 \alpha (M_3 - M_4) + \xi_1 \alpha (S_1 - S_{s1}) \left(\frac{x}{U} - t\right) \exp\left(\frac{-k_1 x}{V_1}\right)$$

$$\text{and} \quad M_4 = M_1 \exp\left(\frac{-k_1 x}{V_1}\right) - M_2.$$

To calculate the concentration of silica in the water returning to the production zone (14), (15), (16) are rewritten in terms of

$$\Phi_f = S_f - S_{s0}.$$

Then

$$\Phi_{ret}(t) = \Phi_f(L, t) \quad (21)$$

where  $L$  is the distance between the production and reinjection zones. Thus, the concentration of the silica, can be obtained as follows:

$$t < t_s$$

$$\Phi_{ret}(t) = 0, \quad (22)$$

$$t_s < t < t_r$$

$$\Phi_{ret}(t) = (S_{s1} - S_{s0}) \exp[\tau(L - Ut)] + (S_1 - S_{s0}) \exp\left[\frac{\sigma L + \omega t}{\delta}\right], \quad (23)$$

$$t > t_r$$

$$\Phi_{ret}(t) = (S_{s1} - S_{s0}) + (S_1 - S_{s1}) \exp\left(\frac{-k_1 L}{V_1}\right). \quad (24)$$

Here  $t_s = \frac{L}{V_0}$  is the time taken for the silica front to travel the distance  $L$ . That is, it is the time taken for the first arrival of injected silica molecules.

### Production Silica

The solution for the concentration of silica in the production zone can now be obtained by integrating equation (3) using standard methods:

$$\Phi_p = \int_0^t [\gamma \Phi_{rel}(\eta) - F(\eta)] e^{\lambda(\eta-t)} d\eta. \quad (25)$$

Substituting (22), (23) and (24) into (25) gives the concentration of silica in the production zone as follows.

$$t < t_s$$

$$S_p(t) = S_{p0} \quad (26)$$

$$t_s < t < t_r$$

$$S_p(t) = S_{p0} + D_1 \exp[\tau(L-Ut)] + D_2 \exp\left[\frac{\sigma L + \omega t}{\delta}\right] - D_3 \exp[-\lambda(t-t_s)] \quad (27)$$

$$\text{where} \quad D_3 = D_1 \exp[\tau(L-Ut_s)] + D_2 \exp\left[\frac{\sigma L + \omega t_s}{\delta}\right],$$

$$D_1 = \frac{\gamma(S_{s1} - S_{s0})}{(\lambda - \tau U)} \quad \text{and} \quad D_2 = \frac{\gamma(S_1 - S_{s1})}{(h + \frac{\omega}{\delta})}$$

$$t > t_r$$

$$S_p(t) = S_{p0} + D_4 \exp[-\lambda(t-t_r)] - D_3 \exp[-\lambda(t-t_s)] + D_5 \{1 - \exp[-\lambda(t-t_r)]\} - k \{f(t) - f(t_r) \exp[-\lambda(t-t_r)]\} \quad (28)$$

where

$$f(t) = \left\{ \frac{m_0}{\lambda} + \frac{m_1}{(\lambda-a)} e^{-at} + \frac{m_2}{(\lambda-2a)} e^{-2at} \right\}$$

$$D_4 = D_1 \exp(\tau(L-Ut_r)) + D_2 \exp\left(\frac{\sigma L + \omega t_r}{\delta}\right)$$

and

$$D_5 = \frac{\gamma}{\lambda} \left[ (S_{s1} - S_{s0}) + (S_1 - S_{s1}) \exp\left(-\frac{k_1 L}{V_1}\right) \right].$$

### Modelling Results

It is assumed that in the reinjection fluid the silica equilibrated to the amorphous silica saturation at the injection temperature of 165° C. The model parameters used in matching the observed changes in the production silica content are listed in Table 1 below.

Table 1. Data Used to Match Silica Breakthrough in PN-26

Average production rate $P$	= 50 kg/s
Initial production silica $S_{p0}$	= 601.2 mg/kg
Injected silica conc. $S_1$	= 710.6 mg/kg
Silica saturation at 165° C $S_{s1}$	= 157.8 mg/kg
Silica saturation at 280° C $S_{s0}$	= 601.2 mg/kg
Silica front velocity $V_1$	= 417.3 d/month
Silica front velocity $V_0$	= 500.2 m/month
Apparent rate constant $k_1^-$	= $2.31 \times 10^{-7} \text{ sec}^{-1}$
Apparent rate constant $k_0^-$	= $3.95 \times 10^{-6} \text{ sec}^{-1}$
Apparent rate constant $k^-$	= $2.65 \times 10^{-6} \text{ sec}^{-1}$
Porosity of silica $\phi_s$	= 0.97
Density of deposited silica $\rho_s$	= 2650 kg/m <sup>3</sup>
Thermal front velocity $U$	= 56 d/month
Porosity of production sector $\phi$	= 0.07
Porosity of fractured zone $\phi$	= 0.07

Equilibrium concentrations of quartz ( $S_s$ ) were calculated from Fournier and Potter (1982). The rate constants were derived from the experimental results of Rimstidt and Barnes (1980). An average value for the rate constant for the production zone was based on the range of measured temperatures (230–280°C) given. The particle velocities  $V_1, V_0$  were calculated by dividing the mass flow rate by porosity and the relevant density.

The following parameters from the previous modelling study (Malate and O'Sullivan, 1990) were used initially:

Mass of water in the production sector  $M_p = 4.0 \times 10^8 \text{ kg}$

Fraction of RI fluid returning  $f = 0.9$

Ratio of thermal properties of rock and water  $\beta = 8.5$ .

The parameters  $\left(\frac{A}{M}\right)_p$  and  $\left(\frac{A}{M}\right)_f$  were then varied to obtain a match to the observed changes in the production silica concentration. By definition the fractured zone is much more fractured than the production sector and a much larger area of rock is available for silica deposition. Therefore the corresponding  $\left(\frac{A}{M}\right)_p$  should be

smaller than  $\left(\frac{A}{M}\right)_f$ . The results for different combinations of production and fractured zone surface areas are shown in Figures 6

and 7. A combination of  $\left(\frac{A}{M}\right)_p = 0.04$  and  $\left(\frac{A}{M}\right)_f = 0.30$  gave reasonable fit to the measured data.

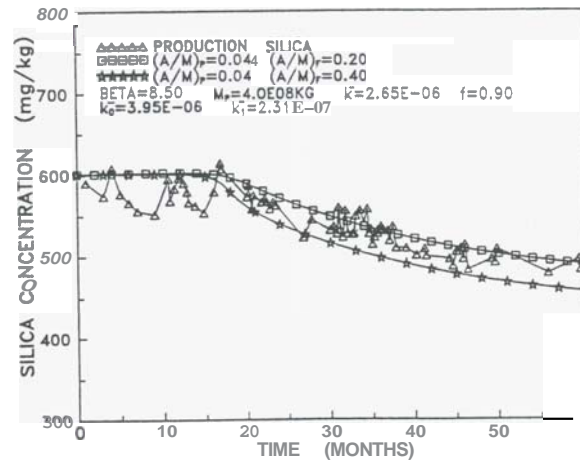


Fig. 6 Production Silica vs Time

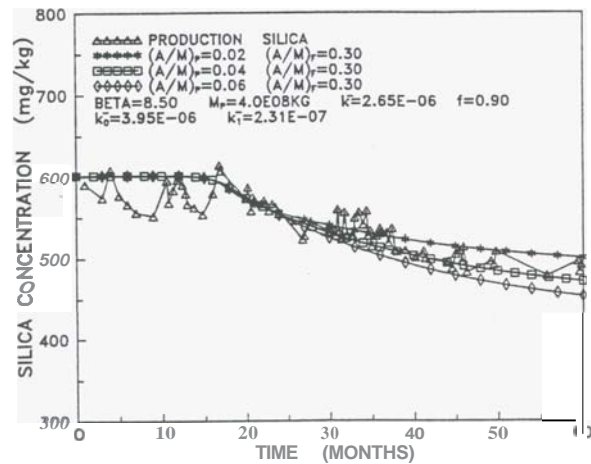


Fig.7 production Silica vs Time

The sensitivity of the model results was also tested by changing the other fitting parameters  $f$ ,  $\beta$  and  $M_p$ . Values off in the interval 0.8 - 0.9 gave a good match of the model results (see Figure 8) to the measured chloride and temperam data, provided that the parameter  $\beta$  was adjusted appropriately (for  $f=0.9$  then  $\beta=8.5$  and for  $f=0.8$



then  $\beta=7.0$  for example). If  $f$  was lowered further, say  $f=0.7$ , it was impossible to match the chloride and temperature data for any choice of  $\beta$ . The same effect was observed with the silica data. For  $f=0.7$  a poor fit was obtained to the observed data. Hence, the best fit values for the parameters  $\beta$  and  $f$ , derived from temperature and chloride models are further validated by the results obtained from the silica model. The fit to the chloride and temperature data was sensitive to the choice of  $M_p$ . However for the silica data the effect of changing  $M_p$  from the initial value is not significant as shown in Figure 9. Therefore the value  $M_p = 4.0 \times 10^8$  kg was used throughout.

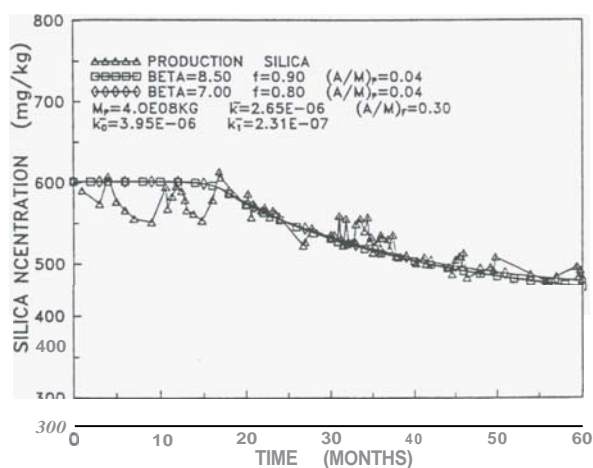


Fig. 8 Production Silica vs Time

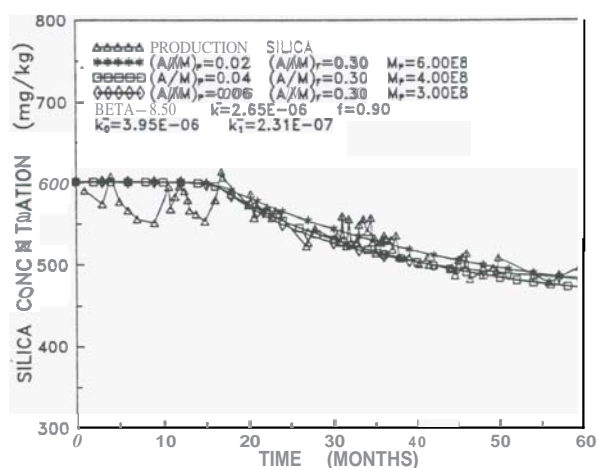


Fig. 9 Production Silica vs Time

The total amount of silica deposited in the production sector can also be determined from the deposition term in (3). The calculation gives a total of 307 tonnes of silica deposited during 60 months. It is also of interest to investigate the deposition of silica in the fractured zone, a plot of reinjection silica with distance for selected time increments is presented in Figure 10. The injected water with  $T_1 = 165^\circ\text{C}$  and  $S_1 = 710 \text{ mg/kg}$  is significantly supersaturated as the silica saturation  $S_{s1}$  is only 158 mg/kg. Therefore as the injected water progresses along the fractured zone silica deposits rapidly. Once the water sweeps heat from the fractured rock and reaches the production sector temperature of  $280^\circ\text{C}$  the silica saturation  $S_{s0}$  is 601 mg/kg. In some cases the silica content may drop below this value before the water is reheated. For example, at early times (5 months), the injected silica concentration declines just to the saturation value of the original fluid temperature of  $280^\circ\text{C}$ , but after 10 months, the silica concentration behind the thermal front has decreased to a value less than saturation conditions at the reservoir temperature. As the reinjection fluid is re-heated, dissolution of quartz takes place beyond the thermal front as the fluid approaches the original equilibrium concentration. This behaviour becomes more pronounced at later times. The corresponding increase in silica specific deposit  $(Q_s - Q_{s0})$  in the fractured zone is displayed in Figure 11. The profiles obtained all give a maximum amount of silica deposited near the reinjection sector. Dissolution of deposited silica takes place ahead of the thermal front at later times.

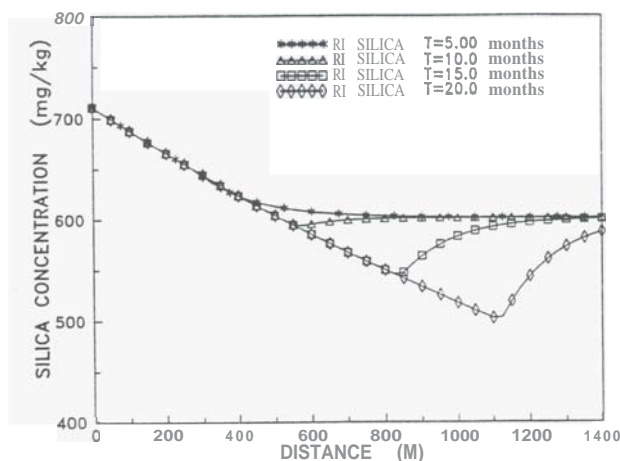


Fig. 10 Reinjection Silica vs Distance

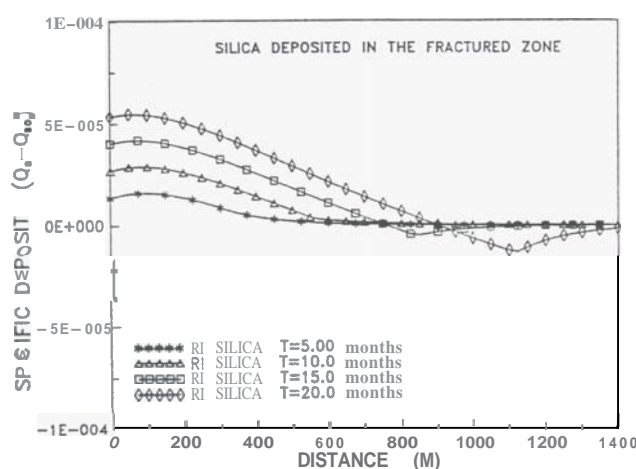


Fig. 11 Silica Specific Deposit vs Distance.

### Summary

It is possible to use the results of the modelling study to carry out a gross silica balance for the whole system. The difference between the production silica content and the amount being reinjected corresponds to approximately 580 tonnes of silica deposited in the surface equipment during 60 months of exploitation. The model for the production sector gives 307 tonnes of silica deposited in the production sector and the transport and deposition model for the fractured zone gives 734 tonnes of silica deposited. These figures can be converted to the following volumetric deposition rates:

Surface equipment	4.0m <sup>3</sup> /month
production sector	2.0m <sup>3</sup> /month
Reinjection sector	5.0m <sup>3</sup> /month

There is very significant deposition of silica in the separator vessels and reinjection pipelines, but the effect of PN-26 cannot be isolated from that of other wells. The figure above for the reinjection sector is about a tenth of the total rate for all wells (51m<sup>3</sup>/month) reported by Harper and Jordan (1985).

### Acknowledgement

The authors wish to acknowledge the management of PNOG-Energy Development Corporation for permission to publish the data in this paper.

### References

- Amistoso, A.E. and Torrejos, A.T. (1986) *Estimation of Pressure Change in the Reservoir and Impact of Reinjection Fluid Returns on Production Wells when the Load increases to 80-85 MWe (Peak)*. PNOG-EDC Internal Report, Philippine National Oil Company - Energy Development Corporation.

Malate and O'Sullivan

**Fournier, R.O. and Potter, R.W. II** (1982) *A revised and expanded silica quartz geothermometer*. Bulletin **Geothermal** Resources Council, **11**, No.10, p. 3-12.

Harper, R.T. (1986) *Silica Breakthrough in PN-26. First Quarter 1986*. PNOC-EDC Internal Report, Philippine National Oil Company - Energy Development Corporation.

Harper, R.T. and Jordan, O.T. (1985) *Geochemical changes in response to production and reinjection for Palinpinon-I geothermal field, Negros Oriental, Philippines*. **7th** New Zealand Geothermal Workshop, University of Auckland, p. 39-44.

Malate, R.C.M. and O'Sullivan, M.J. (1988) *Mathematical Modelling of Silica Deposition*. **Proc. 10th New Zealand Geothermal Workshop**, University of Auckland, p. 257-262.

Malate, R.C.M. and O'Sullivan, M.J. (1990) *Modelling of Chemical and Thermal Changes in Well PN26. Palinpinon, Philippines*, paper presented at 15th Workshop on Geothermal Reservoir Engineering, Stanford University.

Rimstidt, J.D. and Barnes, H.L. (1980) *The Kinetics of Silica-water reactions*. *Geochim. Cosmochim. Acta*, **44**, p 1683-1699.